Isotopic Replacement of Pigments and a Lipid in Chlorosomes from *Chlorobium limicola*: Characterization of the Resultant Chlorosomes†

Yoshinori Kakitani, Ken-ichi Harada, Tadashi Mizoguchi,‡ and Yasushi Koyama*

Faculty of Science and Technology, Kwansei Gakuin University, Gakuen, Sanda 669-1337, Japan

Received December 17, 2006; Revised Manuscript Received March 5, 2007

ABSTRACT: Pigments including bacteriochlorophyll (BChl) *c*, carotenoids, and a trace of BChl *a* together with a lipid, monogalactosyl diglyceride (MGDG), were extracted with chloroform/methanol (1:1 v/v) from an aqueous suspension (50 mM Tris-HCl, pH 8.0) of chlorosomes from *Chlorobium limicola*; other lipids and proteins were left behind in the aqueous layer by funnel separation. The chloroform layer was dried by purging N_2 gas, dissolved in methanol, and rapidly injected into the aqueous layer to reassemble chlorosomes. This technique has been developed to replace one-half of the inherent ^{12}C-BChl *c* by ^{13}C-BChl *c* to identify the intermolecular $^{13}C\cdots{}^{13}C$ magnetic dipole correlation peaks (that are supposed to reduce their intensities to one-fourth by reducing the ^{13}C-BChl *c* concentration into one-half) and to determine the structure of BChl *c* aggregates in the rod elements by means of solid-state NMR spectroscopy. The isotopically replaced chlorosomes were characterized (1) by sucrose density gradient centrifugation, zeta potential measurement, electron microscopy, and dynamic light scattering measurement to determine the morphology of chlorosomes, (2) by ^{13}C NMR spectroscopy, electronic absorption and circular dichroism spectroscopies, and low-angle X-ray diffraction to determine the pigment assembly in the rod elements, and (3) by subpicosecond time-resolved absorption spectroscopy to determine the excited-state dynamics in the pigment assembly. The results characterized the reassembled chlorosomes to have (1) similar but longer morphological structures, (2) almost the same pigment assembly in the rod elements, and (3) basically the same excited-state dynamics in the pigment assembly.

Green sulfur and non-sulfur bacteria have unique antenna complexes called "chlorosomes", which consist of "the rod elements" enveloped by a lipid monolayer. The chlorosomes in *Chlorobium* (*Chl.*)[1] *limicola* and *Chl. tepidum* have been well documented, and the rod element is regarded as a self-assembled cylindrical aggregate of bacteriochlorophyll (BChl) *c*. The structures of chlorosomes and rod elements have been studied extensively in relation to their light-harvesting and photoprotective functions (see, for reviews, refs *1*−*4*).

The above picture of chlorosomes has been developed historically as follows: Chlorosomes were first identified by electron microscopy of thin sections of the cells (*5*), and then, more detailed structural analyses of freeze-fractured samples were performed (*6*). Rod-like structures extending, in parallel, along the long axis of the chlorosomes were clearly demonstrated in *Chl. limicola* (*7*). Most convincingly, the rod elements coming out from chlorosomes that were punctured by osmotic shock were photographed by means of electron microscopy, and a more detailed model for the membrane assembly was presented (*8*). Further topological studies by the use of atomic force microscopy determined the shapes and the dimensions of chlorosomes from various organisms (*9*), and finally, the number of BChl *c* molecules per chlorosome was determined (*10*).

Very recently, however, the above picture of chlorosomes was challenged, and a lamellar model was proposed, instead. Importantly, electron micrographs and low-angle X-ray diffraction exhibited a key diffraction at ∼20 Å in chlorosomes embedded in vitreous ice (*11*). Similar diffractions were observed in the crystals of porphyrins (*12*), supporting the assignment of the ∼20 Å diffraction to the spacing between lamellers consisting of stacked BChl *c* macrocycles (*11*). Further investigations are still necessary to critically evaluate this model.

The rod element has been regarded as an assembly of the cylindrical aggregate of BChl *c* macrocycles: In order to determine the assembly of BChl *c* molecules in the aggregate, a variety of spectroscopic techniques, including electronic absorption and fluorescence, linear dichroism and circular dichroism (CD), infrared and Raman, and magic angle spinning (MAS) nuclear magnetic resonance (NMR) spectroscopies have been applied, and a variety of models has been proposed (ref *3* and references cited therein). However, even the most basic question concerning *the repeating*

† This work has been supported by an Open Research Center Project grant (Research Center of Photo-Energy Conversion) from the Ministry of Education, Culture, Sports, Science, and Technology, Japan (to Y. Koyama). Y. Kakitani has been supported by Research Fellowships of the Japan Society for the Promotion of Science for Young Scientists.

* To whom correspondence should be addressed. Tel/Fax: +81-79-565-8408. E-mail: ykoyama@kwansei.ac.jp.

‡ Current address: Department of Bioscience and Biotechnology, Ritsumeikan University, Nojihigashi, Kusatsu 525-8577, Japan.

[1] Abbreviations: BChl, bacteriochlorophyll; CD, circular dichroism; *Chl.*, *Chlorobium*; DARR, dipolar-assisted rotational resonance; EDTA, ethylenediamine-*N*,*N*,*N*′,*N*′-tetraacetic acid; [E,E], 8-ethyl-12-ethyl bacteriochlorophyll c_F; [E,M], 8-ethyl-12-methyl bacteriochlorophyll c_F; [I,E], 8-isobutyl-12-ethyl bacteriochlorophyll c_F; MAS, magic angle spinning; MGDG, monogalactosyl diglyceride; NMR, nuclear magnetic resonance; NOE, nuclear Overhauser effect; OD, optical density; PDSD, proton-driven spin diffusion; [P,E], 8-propyl-12-ethyl bacteriochlorophyll c_F.

10.1021/bi602586g CCC: $37.00
Published on Web 05/12/2007

subunit forming those aggregates, i.e., either the monomer or the piggy-back dimer (hereafter, simply called "dimer" as well), still remains to be answered. Since the orientation of the BChl *c* molecule is parallel in the monomer-based stacking and antiparallel in the dimer-based stacking, they are sometimes called "the parallel chain model" and "the antiparallel chain model", respectively (*3*). Both the parallel chain model (*13*, *14*) and the antiparallel chain model (*15*, *16*) have been proposed on the basis of ^{13}C NMR spectroscopy and theoretical calculations. The two different kinds of stacking must affect not only the overall assembly of the BChl *c* molecules but also the excited-state dynamics and, as a result, the mechanisms of the light-harvesting and photoprotective functions of chlorosomes. Therefore, it is crucial to find the answer to this question.

When both the parallel and antiparallel stackings form a staircase-like alignment of the macrocycles, the transition dipole−transition dipole interactions probed by electronic absorption and CD spectroscopy as well as the ring current effects probed by ^{1}H and ^{13}C NMR spectroscopy must become very similar, and therefore, it is not straightforward to obtain the answer by these methods, because the orientation of the permanent dipole is not relevant. The most straightforward method is to use a set of short-range interatomic interactions between a pair of macrocycles such as the ^{13}C magnetic dipole-to-^{13}C magnetic dipole interactions.

Most recently, we have succeeded in determining the stacking of the BChl *c* molecules in in vitro aggregates consisting of an isomeric mixture of BChl *c* extracted from *Chl. limicola* by the use of intermolecular ^{13}C···^{13}C correlation peaks in the proton-driven spin diffusion spectra (PDSD) (*17*). In order to extract the intermolecular ^{13}C···^{13}C correlation peaks, we have used the following strategy: Upon dilution of ^{13}C-BChl *c* with ^{12}C-BChl *c* in a 1:1 ratio, the *intramolecular* correlation peaks decrease in intensity into one-half (the number of the covalently bound ^{13}C−^{13}C pairs), whereas the *intermolecular* correlation peaks, into one-fourth (the number of the intermolecular nonbonding ^{13}C···^{13}C pairs out of the ^{13}C···^{13}C, ^{13}C···^{12}C, ^{12}C···^{13}C, and ^{12}C···^{12}C pairs). In order to apply this dilution method to the case of *chlorosomes*, however, we need to make cylindrical BChl *c* aggregates containing a 1:1 mixture of ^{13}C-BChl *c* and ^{12}C-BChl *c* forming the rod elements and to envelop them in the lipid monolayer of monogalactosyl diglyceride (MGDG). We used a method similar to that of Matsuura and co-workers (*18*), who succeeded in the preparation of a chlorosome-like structure by (i) the extraction of the lipids and pigments with a chloroform/methanol/water mixture (1:1:2), (ii) dissolving the dried chloroform extract in methanol, and (iii) the injection of the methanol solution into a phosphate buffer. The resultant aggregates showed a red-shifted Q_y absorption, strong linear dichroism, and a rod-like structure in an electron micrograph. In our preparation, however, we directly used the aqueous layer after extraction (instead of a pure buffer solution), in the reassembly of chlorosomes, in order to make the composition of the aqueous phase as close as possible to that in the intact chlorosomes.

More specifically, we prepared two different kinds of chlorosomes, one from the cells grown in the ^{13}C-enriched medium ("^{13}C-chlorosomes") and the other from the cells grown in the medium of natural abundance isotopic composition ("^{12}C-chlorosomes"). Then, we extracted BChl *c*, carotenoids, and MGDG with the above-mentioned organic solvent from both ^{13}C- and ^{12}C-chlorosomes, mixed with each other in a 1:1 ratio, dried and dissolved into methanol, and injected the solution to the aqueous phase obtained from chlorosomes. Hereafter, we will call the resultant chlorosomes "reassembled chlorosomes".

In the present investigation, we aimed at the characterization of the reassembled chlorosomes and took the following three steps to determine their structural and excited-state properties by the use of the following experimental techniques, (a)−(h). First, we examined how the morphology of the reassembled chlorosomes compares or contrasts to that of the intact chlorosomes: We compared (a) their densities by sucrose density gradient centrifugation, (b) the surface charges of their lipid envelopes by zeta potential measurement, (c) their structures by electron microscopy, and (d) their size distributions by dynamic light scattering. Second, we examined the pigment assemblies in the rod elements: We determined (e) the ^{13}C magnetic dipole interactions by solid-state NMR spectroscopy, (f) the Q_y transition dipole−transition dipole interactions by electronic absorption and CD spectroscopies, and (g) the regular atomic distances by low-angle X-ray diffraction. Finally, we examined (h) the excited-state dynamics by subpicosecond time-resolved absorption spectroscopy.

We have addressed the following three specific questions: (1) How can the morphology of the reassembled chlorosomes be characterized in comparison to the intact chlorosomes? (2) How can the BChl *c* aggregates forming the rod elements be characterized in comparison to those in the intact chlorosomes? Can any conclusion be drawn concerning the monomer-based or the dimer-based stacking by the use of the set of data obtained? (3) How can the excited-state dynamics be characterized? Can any relevance be found concerning the light-harvesting or photoprotective function of chlorosomes?

MATERIALS AND METHODS

Dissociation and Reassembly of Chlorosomes. The cells of *Chl. limicola* f. sp. *thiosulfatophilum*, of natural-abundance and ^{13}C-substituted isotopic composition, were grown anaerobically at 27 °C in the dim light in the medium of Wahlund et al. (*19*), the details of which were described elsewhere (*17*).

First, chlorosomes were prepared from the cells mentioned above according to the method of Gerola and Olson (*20*): The cells were suspended in a buffer (pH 7.4) containing 10 mM potassium phosphate, 10 mM sodium L-ascorbate, and 2 M NaSCN and then disrupted four times by the use of a French press (pressure 1150−1250 kg·cm^{-2}). The suspension was centrifuged at 31000*g* for 30 min, and the supernatant was subjected to sucrose density gradient centrifugation (200000*g* for 18 h) to obtain "intact chlorosomes", the details of which in *Chl. tepidum* were described elsewhere (*21*); some modifications were made in the technique of sucrose density gradient centrifugation of the chromatophores from the cells cultured in the ^{12}C and ^{13}C media. Second, the chlorosomes thus obtained were dissociated into chloroform-soluble and methanol/water-soluble components, and then, the two components were mixed to

form "reassembled chlorosomes": More precisely, to a chlorosome aqueous suspension (the concentration, OD = 300 cm^{-1} at the Q_y absorption maximum, 748 nm; and the volume, 0.15 mL), a chloroform/methanol (1:1 v/v) mixture (2 mL) and, then, an aqueous solution [15 mL; containing 50 mM Tris-HCl (pH 8.0) and 1 mM ethylenediamine-*N*,*N*,*N*′,*N*′-tetraacetic acid (EDTA)] were added to obtain the chloroform and the aqueous layers. [Thin-layer chromatography and electronic absorption spectroscopy showed that the chloroform layer contained BChl *c*, BChl *a*, carotenoids, and MGDG, whereas the aqueous layer contained other lipids.] Finally, the chloroform layer was dried by purging N_2 gas, dissolved into methanol, and divided into six aliquots; the aqueous layer was also divided into six aliquots. Each aliquot of the methanol solution (0.2 mL) was injected *rapidly* at ~20 °C into that of the aqueous layer to form reassembled chlorosomes.

Techniques for Characterization of the Intact and Reassembled Chlorosomes. (a) Sucrose Density Gradient Centrifugation. The intact or reassembled chlorosomes (the concentration, OD = 100 at the Q_y absorption maximum) were charged onto the sucrose gradient layers (0% 6 mL with chlorosomes, 30−40% gradient 24 mL, and 50% 6 mL) containing 50 mM Tris-HCl buffer (pH 8.0) and 1 mM EDTA and centrifuged for 18 h at 200000*g*.

(b) Measurement of Zeta Potential. The zeta potentials of the intact and reassembled chlorosomes (the concentration, OD = 1 at the Q_y absorption maximum) were measured at 25 °C, by the use of a glass cell on a Otsuka Electronics ELS-Z2 zeta-potential and particle-size analyzer equipped with a diode laser.

(c) Electron Microscopy. Electron micrographs were taken for both chlorosomes in suspension (the concentration, OD = 1 at the Q_y absorption maximum) that were mounted on a grid coated with a collodion film and negatively stained with 4% phosphotungstic acid (pH 7.4; Wako Pure Chemical Ind., Japan), by the use of a Hitachi H-7650 transmission electron microscope at an electron-accelerating voltage of 100 kV.

(d) Dynamic Light Scattering. The size distribution of the intact/reassembled chlorosomes was measured at 25 °C by the use of a 1 cm cuvette on a Otsuka Electronics ELS-Z2 zeta-potential and particle-size analyzer.

(e) NMR Spectroscopy. The ^{13}C magnetic dipole correlation spectra were recorded for each chlorosome paste (OD·V = 1600 cm^{-1}·mL at the Q_y absorption maximum) placed in a rotor (o.d. 4 mm) on a JEOL JNM-ECA 600 FT-NMR spectrometer (the magnetic field, 14.096 T; and the resonance frequencies, 150.9 MHz for ^{13}C and 600.17 MHz for ^{1}H). The dipolar-assisted rotational resonance (DARR) technique (*22*) was used to obtain two pairs of spectra in Figure 5 (the upper and the lower panels) with cross-polarization; the contact time, both 2.0 ms; the mixing time, 200 and 100 ms; the MAS rate, 8 and 10 kHz; and data accumulation, 8 and 17 h, respectively. The temperature of each sample was estimated to be around 30 °C.

(f) Electronic Absorption and CD Spectroscopies. Electronic absorption spectra were recorded at 25 °C by the use of a Hitachi U-2000 spectrophotometer and a 1 cm quartz cell for both chlorosomes (the concentration, OD = 1 at the Q_y absorption maximum). CD spectra were recorded by the use of a JASCO J-720W spectropolarimeter under the N_2 atmosphere.

(g) Measurement of Low-Angle X-ray Diffraction. X-ray diffraction patterns were measured with a Rigaku RINT 2100/PC X-ray diffractmeter for both chlorosomes in a reflection geometry. Special attention was paid in the handling of chlorosome samples to keep the water content: The sample mounted on a ground glass was kept wet by constant addition of water; the mount together with a tiny water bottle was placed in an acrylic housing having a Teflon lid and a Teflon window to pass the X-ray beams (in and out). The housing was tightly sealed.

(h) Subpicosecond Time-Resolved Absorption Spectroscopy. (1) Samples. The intact or reassembled chlorosomes were suspended, in a 50 mM Tris-HCl buffer (pH 8.0) containing 1 mM EDTA, at a concentration of OD = 6 cm^{-1} at the maximum of the Soret absorption. The sample suspension was circulated between a 1 mm flow cell and an ice-cooled reservoir (20 mL) by the use of a peristaltic pump (the linear speed in the cell, 7 cm·s^{-1}). The stationary-state electronic absorption spectra were recorded on a Hitachi U-2000 spectrophotometer before and after each measurement; no photodegradation was identified at all.

(2) Setup and Experimental Conditions. A Quantronix regenerative amplifier (Integra) that was seeded by a Coherent mode-locked Ti:sapphire laser (Vitesse) delivered 801 nm pulses (100 fs, 1 kHz, 1.5 mJ·$pulse^{-1}$), which was split into two components by the use of a 4:1 beam splitter. The major component was sent to a Quantronix optical parametric amplifier (Topas) to generate 454 or 455 nm pump pulses (100 fs, 1 kHz), whose energy was attenuated to 1.2−1.4 μJ·$pulse^{-1}$ at the sample cell; the pumping energy corresponds to a photon density of 2.6×10^{14} photon·cm^{-2}·$pulse^{-1}$. The minor component was focused into a 1 cm water cell to generate white-continuum probe pulses. The polarization of the pump beam was set to the magic angle (54.7°) with respect to the horizontally polarized probe beam. The probe beam was led into a 1 mm optical fiber and then into a polychromator (SPEX 270M equipped with a 150 line·mm^{-1} grating) and focused onto a liquid nitrogen-cooled CCD detector (SPEC-10:100F; Princeton Instruments Inc.) using only 1340 × 20 pixels for fast read-out. For each pair of pump and probe pulses, the difference spectrum of "with pump" minus "without pump" was calculated, and a total of 1000 difference spectra were accumulated at each delay time.

The cross-correlation between the pump and probe pulses as well as the dispersion in the probe pulse was determined by means of a nonresonant optical Kerr signal using a 1 mm quartz plate. The full width at half-maximum of the cross-correlation trace between the pump and the probe pulses was determined to be 140 fs. A calibration curve was then obtained by the least-squares fitting of a polynomial function to the dispersion data, and it was used as a standard for the dispersion correction of the observed time-resolved spectra; an error of the dispersion correction was estimated to be ±20 fs.

RESULTS AND DISCUSSION

Morphology of the Intact and Reassembled Chlorosomes. (a) Densities Determined by Sucrose Density Gradient Centrifugation. Figure 1 shows the results of centrifugation

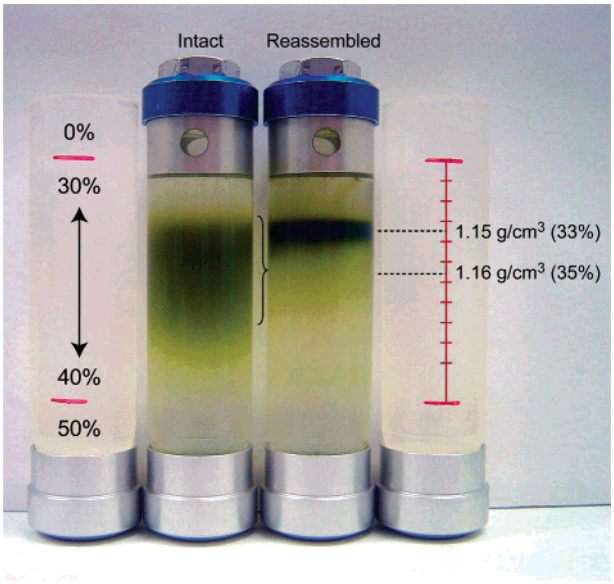

FIGURE 1: Densities of the intact and reassembled chlorosomes determined by sucrose density gradient centrifugation. Chlorosomes were deposited on the three steps of sucrose layers (0%, 30−40%, and 50%) containing 50 mM Tris-HCl (pH 8.0) and 1 mM EDTA and centrifuged for 18 h at 200000*g*.

of the intact and reassembled chlorosomes deposited on the three steps of sucrose layers (0%, 30−40%, and 50%) containing 50 mM Tris-HCl (pH 8.0) and 1 mM EDTA. The intact chlorosomes show densities in the range of 1.15−1.17 g·cm^{-3} (centered around 1.16 g·cm^{-3}), whereas the reassembled chlorosomes, a density of 1.15 g·cm^{-3}. This is actually the definition of our "intact" and "reassembled" chlorosome preparations.

The broad range of density seen in the intact chlorosomes may originate from the inhomogeneous light intensity during the cell growth of *Chl. limicola* in a Rue bottle. The light intensity should be higher for the cells growing on the surface, whereas it should be lower for the cells growing in the central part of the bottle due to the *self-shadowing* effect. The isomeric and epimeric compositions can vary depending on the light intensity, and as a result, the packing of BChl *c* molecules in the aggregates forming the rod element may vary slightly, depending on the cells grown under the different light intensities:

It was found that the composition of isomers, concerning the side chains attached to the C8 and C12 positions (see Scheme 1), could vary depending on the light intensity in *Chl. limicola* (*23*). With decreasing the light intensity, 8-ethyl-12-methyl bacteriochlorophyll c_F ([E,M]) and 8-ethyl-12-ethyl bacteriochlorophyll c_F ([E,E]) isomers decrease in the amount, whereas 8-propyl-12-ethyl bacteriochlorophyll c_F ([P,E]) and 8-isobutyl-12-ethyl bacteriochlorophyll c_F ([I,E]) increase. Therefore, the isomeric composition can vary depending on the light intensity.

It was also found that BChl *c* isomers having a smaller side chain at the C8 position predominantly take the *R*-configuration, whereas those having a larger side chain, the *S*-configuration (*24*). Further, the genomic analysis of the C3^1 hydration reaction showed that the enzymes *bchF* and *bchV* are involved in the synthesis of *R*- and *S*-bacteriochlorophyllides, respectively, in the biosynthetic pathways of BChl *c* homologues (*25*). Interestingly, we have

Scheme 1

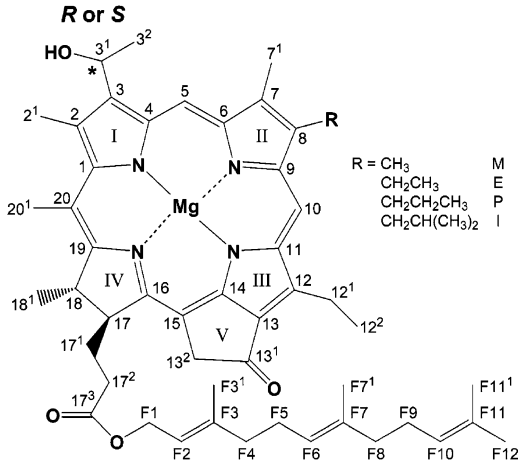

found that (3^1*R*)-BChl *c* having small side chains, i.e., *R*[E,E] and *R*[P,E], tend to form the dimer-based stacking absorbing at 705 and 745 nm, respectively (*26*, *27*), whereas (3^1*S*)-BChl *c* having a bulky side chain, *S*[I,E], tends to form the monomer-based stacking (*28*, *29*) absorbing at 740 nm. Similar findings were made in the case of BChl *e* (*30*).

Thus, the intact chlorosomes from the cells grown under various light intensities may have different densities due to different molecular packing and give rise to such a broad band in the sucrose density gradient centrifugation.

In the case of the reassembled chlorosomes, the isomeric and epimeric composition of BChl *c* homologues may be averaged and become almost the same, during the processes of extraction and reassembly of the pigment molecules. Most probably, the packing of the BChl *c* molecules in the aggregate are homogeneous, giving rise to such a sharp density distribution in the sucrose density gradient centrifugation.

The averaged density of the reassembled chlorosomes (1.15 g·cm^{-3}) is lower than that of the intact chlorosomes (1.16 g·cm^{-3}). This difference may originate from the processes of generating aggregates to form the rod elements: Most probably, the reassembled chlorosomes were generated immediately after the injection of a mixture of BChl *c* homologues and MGDG into the aqueous phase. On the other hand, the intact chlorosomes must be formed gradually during the growth of the cells. In the former, the BChl *c* isomers may be assembled like rapidly condensed amorphous solids, while in the latter, they may be assembled in a more organized and equilibrated way like growing two-dimensional crystals of slightly different compositions.

(*b*) *Surface Charges As Determined by Zeta Potential.* The zeta potential is defined by the effective charges on the gliding surface of a spherical electrophoretic unit, consisting of the charges on each chlorosome and the surrounding counter charges forming a diffusing double layer, both in reference to the zero field defined at a long distance where the electric neutrality of the entire sphere is realized. It can be determined by the Doppler effect in the light scattering from the electrophoretic units that are moving in the external electric field.

Figure 2 shows the results of zeta potential measurements. The excellent agreement in the maxima of the zeta potential profiles between the intact and reassembled chlorosomes

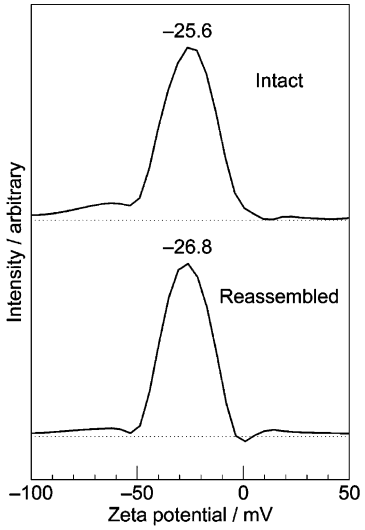

FIGURE 2: Surface charges of the intact and reassembled chlorosomes as determined by measurement of zeta potential (see the text for the principle).

strongly suggests that, in both chlorosomes, the BChl *c* aggregates to form the rod elements are enveloped by the same MGDG lipid monolayer most probably with the hydrophilic galactosyl and acyl groups on the outer side. The slightly more negative value of the reassembled chlorosomes may reflect their elongated structure in comparison to the intact chlorosomes as will be shown in (c) and (d).

(*c) Structures Observed by Transmission Electron Microscopy.* Figure 3 shows the electron micrographs of the intact and reassembled chlorosomes. The shape of the former is a round and smooth spheroid, whereas that of the latter is an elongated spheroid forming a spiral. Such spiral structures were actually found in the intact chlorosomes from *Chl. pheobacteroides* and *Chl. vibrioforme* (see Figure 2 of ref 9), as well. The size of the reassembled chlorosomes (175 nm × 50 nm) is much larger than that of the intact chlorosomes (100 nm × 40 nm). Both chlorosomes tend to stick together to form an aggregate, on the collodion film, possibly due to hydrogen bonding among the galactosyl groups and water molecules.

The different shapes and sizes of the intact and reassembled chlorosomes may also originate from the different processes in the formation of chlorosome structures as mentioned in (a). In the formation of the intact chlorosomes, there may be biological controll to make their shapes homogeneous. In the formation of the reassembled chlorosomes, on the other hand, there can be a competition between the growth of pigment aggregates to form the rod elements and the coverage of the rod elements by MGDG in an inhomogeneous microenvironment. In this process, the pigment aggregation may be sometimes faster than the coverage by MGDG to form larger rod elements. In the electron micrographs, we also see some naked aggregates (see the inset) forming rod-like structures, supporting this interpretation. No such naked structures were seen at all in the intact chlorosomes.

(*d) Size Distributions Determined by Dynamic Light Scattering.* The dynamic light scattering is defined by the fluctuation of light scattering due to the Brownian motion of particles. In the analysis, the autocorrelation function of fluctuation between times t and $t + \tau$ is first calculated for

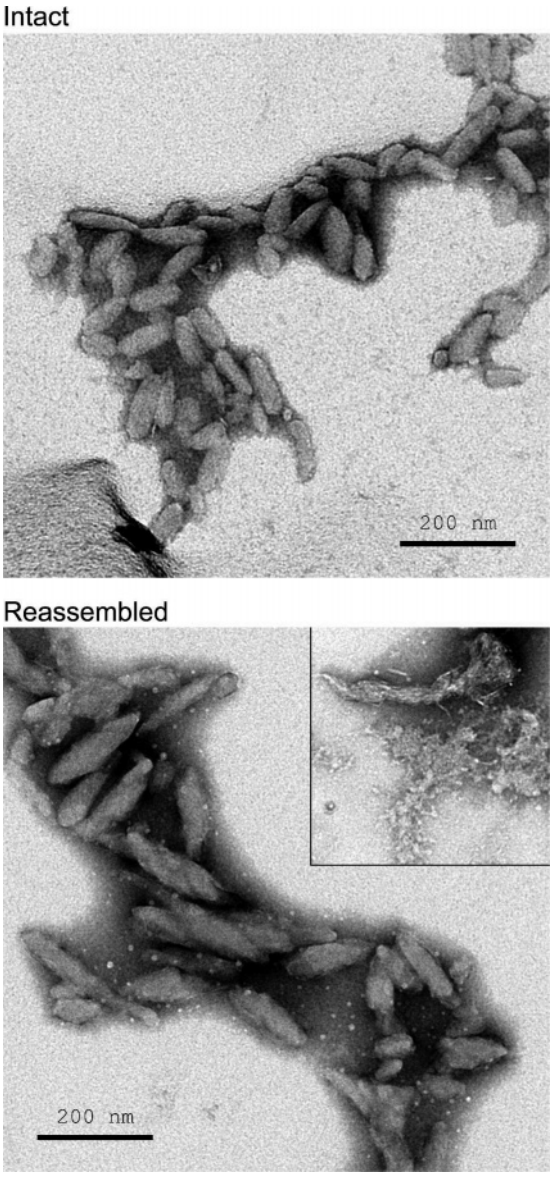

FIGURE 3: Structures of the intact and reassembled chlorosomes observed by electron microscopy. Chlorosomes were mounted on a grid coated with a collodion film and negatively stained with 4% phosphotungstic acid (pH 7.4). Electron micrographs were taken at an electron-accelerating voltage of 100 kV. Inset: naked rod element-like structures seen in the case of reassembled chlorosomes.

various τ values; it decreases exponentially as a function of τ. By the use of the decay time constant thus determined, the translational diffusion coefficient was then calculated. Finally, the distribution of the Stokes radii was calculated by the use of the Einstein−Stokes equation assuming a spherical structure.

Figure 4 presents the profiles of size distribution that were determined by dynamic light scattering: The diameter at the maximum population is ∼80 nm in the intact chlorosomes, while it is ∼190 nm in the reassembled chlorosomes. The pair of diameters were roughly parallel to the lengths of the long axes in the intact and reassembled chlorosomes, i.e., ∼100 and ∼175 nm, respectively, that were measured by the use of the electron micrographs [see (c)].

Now, we are going to discuss (speculate) a possible reason for the different sizes between the intact and reassembled chlorosomes: The size of the reassembled chlorosomes may

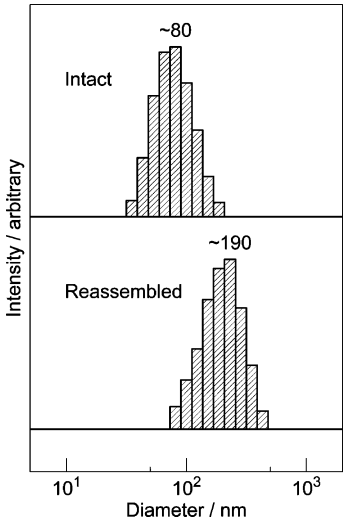

FIGURE 4: Size distributions in the intact and reassembled chlorosomes as determined by analysis of dynamic light scattering assuming spherical structures (see the text for the principle).

be determined by the relative amounts of MGDG vs BChl *c*, because the formation of the reassembled chlorosomes can be the result of competition between the growth of pigment aggregates to form the rod elements and the coverage of them by MGDG as mentioned above.

In the procedure of reassembling chlorosomes, we extracted both BChl *c* and MGDG with chloroform/methanol. After drying the extract, dissolving into methanol, and injecting the solution to the aqueous layer after funnel separation, we noticed that some white material was stuck to the wall of the glass test tube. Since the pigments (BChls and carotenoids) were readily soluble to methanol, we suspect the remaining material can be the lipid, MGDG. Therefore, the amount of MGDG might be smaller than that of BChl *c*. We even observed *naked* rod elements that were not enveloped by MGDG at all. It is likely that the larger size of the reassembled chlorosomes is due to the relatively smaller amount of MGDG available.

Pigment Assembly in the Aggregates Forming the Rod Elements in the Intact and Reassembled Chlorosomes. (e) ^{13}C Magnetic Dipole Interactions Probed by Solid-State NMR Spectroscopy. In the ^{13}C−^{1}H DARR MAS ^{13}C NMR spectroscopy, a radio-frequency field is applied not on ^{13}C but on ^{1}H to recouple the ^{13}C−^{1}H dipolar interactions to achieve the dipolar line broadening and to produce spectral overlap necessary to conserve energy in the ^{13}C−^{13}C polarization transfer (*22*).

Figure 5 (upper pair of panels) compares the DARR spectra of the intact and reassembled chlorosomes both consisting of 100% ^{13}C-BChl *c* (both spectra were symmetrized by averaging the off-diagonal peaks). Here, the spinning frequency was lowered (8 kHz) to minimize the evaporation of water. Many correlation peaks from the intact and reassembled chlorosomes (100% ^{13}C-BChl *c*) are similar to each other, a fact which strongly suggests that the stackings of the macrocycles are basically the same. However, it is also clear that the intact chlorosomes give rise to a larger number of carbon−carbon (both intramolecular ^{13}C−^{13}C and intermolecular ^{13}C···^{13}C) correlation peaks than the reassembled chlorosomes (see the arrangement of peaks along ∼35 and ∼175 ppm, for example), a fact which

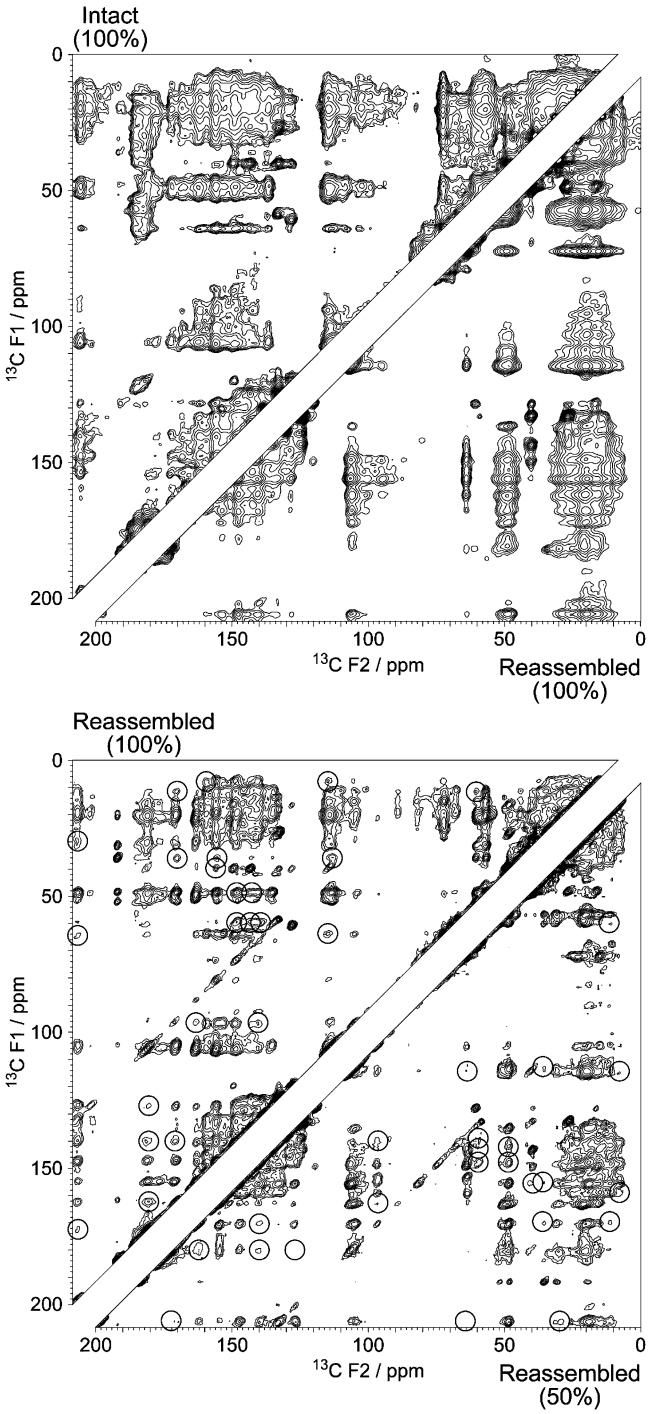

FIGURE 5: (Upper pair of panels) DARR spectra of the intact and reassembled chlorosomes both containing 100% ^{13}C-BChl *c*. Conditions: cross-polarization; contact time, 2.0 ms; mixing time, 200 ms; MAS rate, 8 kHz; data accumulation, 8 h. (Lower pair of panels) DARR spectra of the reassembled chlorosomes containing 100% and 50% ^{13}C-BChl *c*. Intermolecular ^{13}C···^{13}C correlation peaks whose intensity decreased to about one-fourth by dilution to one-half are circled. Conditions: cross-polarization; contact time, 2.0 ms; mixing time, 100 ms; MAS rate, 10 kHz; data accumulation, 17 h.

suggests that the intact chlorosomes contain a larger number of lipids than the reassembled chlorosomes. Thus, some lipids may have been lost in the procedure of separation and reassembly to form chlorosomes using the chloroform and aqueous components.

Figure 5 (lower pair of panels) compares the DARR spectra of the reassembled chlorosomes containing 100% and

50% ^{13}C-BChl *c*. Here, a larger number of well-resolved correlation peaks are observed with a higher spectral resolution, probably due to a higher spinning frequency (10 kHz). Those peaks whose intensities are substantially reduced (to about one-fourth) on going from 100% to 50% BChl *c* are assigned to the intermolecular ^{13}C···^{13}C correlation peaks (indicated by circles). Thus, we have achieved our goal, and those peaks will be used to determine the pigment assembly in the reassembled chlorosomes. The structural analyses by simulation of the nearest-neighbor intermolecular carbon−carbon close contacts, with distances of 4−6 Å, are now in progress. The distribution of those *intermolecular* correlation peaks suggests a pigment assembly that is somewhat similar to that found in the in vitro aggregates of the BChl *c* isomeric mixture in the solid state, i.e., the coexistence of the dimer-based and pseudo-monomer-based stackings (*17*).

Even at the present stage, we have obtained an answer to the issue concerning the repeating subunit of BChl *c* aggregates is either the monomer or the piggy-back dimer: In a previous investigation (*26*), we determined the structure of a higher aggregate of *R*[E,E] suspended in chloroform by the use of the aggregation shifts of the ^{13}C and ^{1}H signals (simulated by the calculation of the ring current effects) and 3d F1 ^{13}C-edited F3 ^{13}C-filtered heteronuclear single-quantum nuclear Overhauser effect (NOE) spectroscopy applied to a 1:1 mixture of ^{13}C-BChl *c* and ^{12}C-BChl *c* (analyzed in terms of intermolecular ^{1}H−^{1}H NOE correlations). As a result, we have shown that the piggy-back dimer can give rise to a large splitting of the C5 signal due to two different conformations of the hydroxyethyl groups that coordinate to a pair of Mg atoms; the different conformations can cause different types of intermolecular ^{13}C···^{13}C contacts and, as a result, different ^{13}C chemical shift values (see Figures 3 and 4 as well as Table 1 of ref *26*).

Figure 6 shows a pair of strip charts from the DARR spectra of the intact and reassembled chlorosomes. The large splittings of the C5-related signals clearly show that both BChl *c* aggregates, forming the rod elements in the intact and reassembled chlorosomes, consist of the piggy-back dimers.

(f) Interactions among the Q_y Transition Dipoles Probed by Electronic Absorption and CD Spectroscopies. Figure 7 compares the electronic absorption spectra of the intact and reassembled chlorosomes. The Q_y absorption band of the intact chlorosomes can be characterized as follows in comparison to that of the reassembled chlorosomes. (i) The maximum of the Q_y absorption band appears at 748 nm in the former, whereas it appears at 749 nm in the latter: the red shift of the Q_y absorption due to the aggregate formation is slightly smaller in the intact chlorosomes than in the reassembled chlorosomes. (ii) When the intensity of the Q_y absorption is normalized to 1, the relative intensity of the Soret absorption is 0.71 in the former and 0.76 in the latter; therefore, the relative intensity of the Q_y absorption is higher in the intact chlorosomes than in the reassembled chlorosomes. (iii) The width of the Q_y absorption is smaller in the intact chlorosomes (43 nm) than that in the reassembled chlorosomes (51 nm). In the reassembled chlorosomes, the assembly of macrocycles in the cylindrical aggregates of BChl *c*, forming the rod elements, may be less organized and give rise to a wider size distribution as far as the interactions of the Q_y transition-dipole moments are concerned. The shoulders appearing around 504 nm in both chlorosomes are ascribable to the $1B_u^+ \leftarrow 1A_g^-$ absorption of carotenoids, which may play an important role in stabilizing the aggregate structure of BChl *c* (*31*).

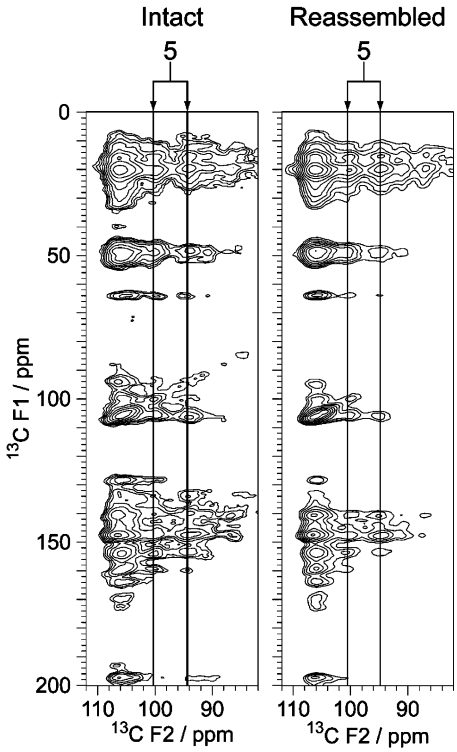

FIGURE 6: A pair of strip charts from the DARR spectra of the intact and reassembled chlorosomes. The large splitting of the C5-related peaks indicates that the BChl *c* aggregates forming the rod elements in the chlorosomes consist of the piggy-back dimers (see the text for the basis of this interpretation).

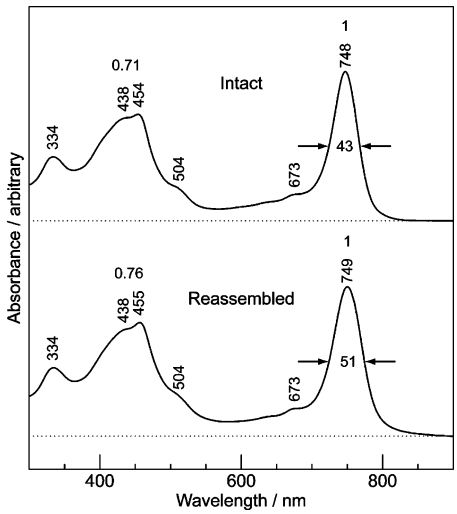

FIGURE 7: Electronic absorption spectra of the intact and reassembled chlorosomes. The width of the Q_y absorption and the intensity of the Soret absorption relative to that of Q_y absorption are indicated for each sample together with the wavelengths of absorptions.

Thus, the overall spectral patterns are very similar to each other, an observation which indicates that the pigment assembly is basically the same between the intact and reassembled chlorosomes.

Figure 8 shows the CD patterns of the intact and reassembled chlorosomes in the longer wavelength region.

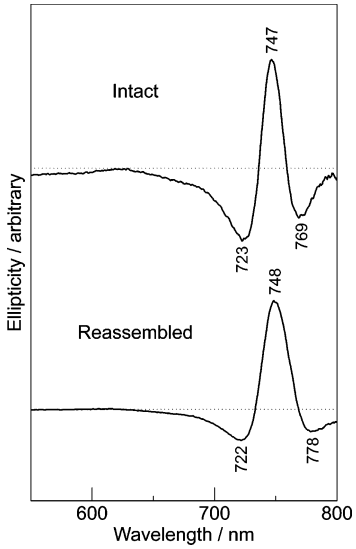

FIGURE 8: CD spectra of the intact and reassembled chlorosomes in the longer wavelength region. The CD pattern of the Q_y absorption with signs (−, +, −) indicate the formation of a left-handed cylindrical aggregate of BChl *c* (see the text).

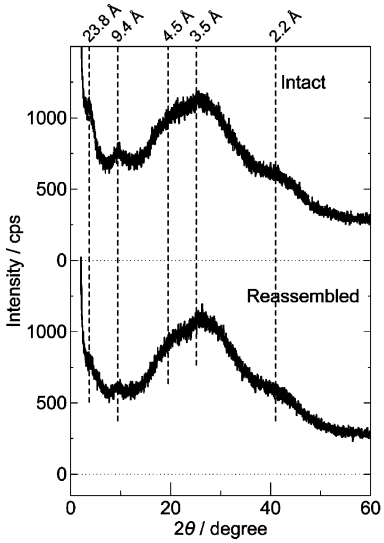

FIGURE 9: Low-angle X-ray diffraction patterns of the intact and reassembled chlorosomes recorded in a reflection geometry. To keep the water content, each sample was mounted on a ground glass, which was covered by an acrylic housing with a Teflon lid and a Teflon window to pass the X-ray beams (in and out).

The CD pattern of the Q_y absorption with signs (−, +, −) from the higher to the lower energies is characteristic of "protein-free" chlorosomes (*32*). A very similar CD pattern was obtained in chlorosomes from *Chl. tepidum* (*33*) that were prepared following the method of Gerola and Olson (*20*). This particular CD pattern is a sum of type I and type II according to the definition of Griebenow et al. (*32*).

On the basis of recent theoretical calculations (*34*, *35*), it has been concluded that both the intact and reassembled chlorosomes form a cylindrical aggregate with the transition dipoles inclined in reference to its long axis. Our preliminary calculations showed that this spectral pattern can be simulated in terms of a left-handed cylindrical aggregate (Kakitani et al., unpublished results).

(g) Regular Atomic Arrangements Probed by Low-Angle X-ray Diffraction. Figure 9 compares the profiles of low-angle X-ray diffraction between the intact and reassembled chlorosomes. One of the most important findings, in the present investigation, is that the water content was the key to reproduce the particular diffraction pattern and, therefore, to keep the particular aggregate structure in the rod elements. When the chlorosome preparations have been dried out, peaks at 2.2, 3.5, 9.4, and 23.8 Å completely disappear, and only two peaks remain at 4.5 and 11.5 Å (data not shown). This change in the diffraction pattern, upon removal of water, took place in both the intact and reassembled chlorosomes. The latter two peaks were actually observed in the in vitro aggregate of a mixture of BChl *c* homologues in the solid state, whose structures were determined in our previous investigation (*17*).

The diffraction patterns of the intact and reassembled chlorosomes, in the present preparation, are almost indistinguishable, a fact which indicates that the basic atomic skeletons in the pigment assembly are almost identical as far as the regular atomic arrangements are concerned.

We have tried to interpret the diffraction patterns in terms of a dimer-based stacking of the BChl *c* macrocycles based on the model we proposed in the in vitro aggregate mentioned above (*17*). We newly introduced water molecules to form a hydrogen-bonding network including the Mg atom as well as the keto C═O and the hydroxyethyl OH groups in the macrocycle. The attempt led us to propose the following *tentative* assignments of those diffraction peaks: (i) 2.2 Å, the regular oxygen-to-oxygen arrangement forming strong C═O···HO hydrogen bondings; (ii) 3.5 Å, regular magnesium-to-oxygen arrangement forming the Mg··· hydroxyethyl OH coordination bonds; (iii) 4.5 Å, regular carbon-to-carbon arrangements between the neighboring methyl/methylene···methyl/methylene van der Waals contacts; (iv) 9.4 Å, regular *intercolumn* magnesium-to-magnesium arrangement between the same type of BChls in the dimer; and (v) 23.8 Å, unassigned diffraction peak.

(h) Excited-State Dynamics Probed by Time-Resolved Absorption Spectroscopy. Figure 10 shows subpicosecond time-resolved absorption spectra of the intact and reassembled chlorosomes. The ground-state spectra are also shown on the top for comparison. The time-dependent changes in the spectral pattern are very similar to each other. They can be characterized as follows: (i) Immediately after excitation at the Soret absorption (454 nm), stimulated emission takes place from this particular state giving rise to a peak (∼462 nm), which is sharper and red shifted in comparison to the above ground-state Soret absorption. (ii) At around 0.20 ps after excitation, a broad absorption band peaked around 550 nm, ascribable to the T_1 state (see ref *21*), appears together with a shoulder (736 nm) and the main component (770 nm) of the Q_y emission. (iii) At around 20 ps after excitation, the above higher energy shoulder component disappears, and the main component (770 nm) stays.

The above spectral changes can be interpreted in terms of the following excited-state dynamics: (i) Immediately after excitation, stimulated emission takes place from the Soret excited state, to which the BChl *c* molecules were excited. (ii) During this process of stimulated emission, the singlet−homofission reaction takes place to generate a pair of T_1 states, which is followed by the triplet−triplet annihilation reaction to generate a hot Q_y state slightly higher in energy

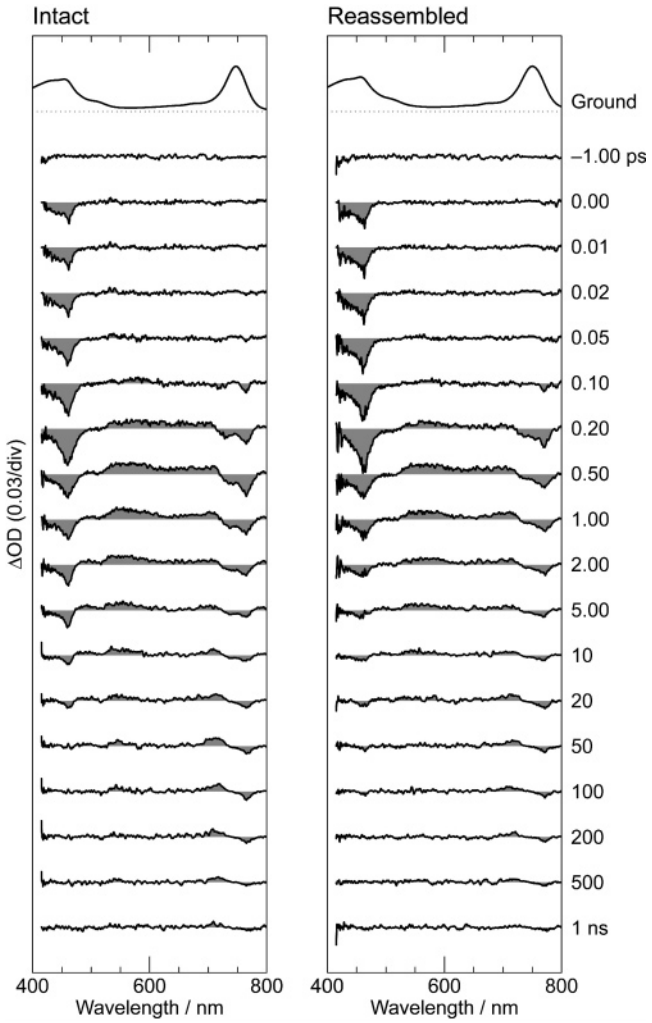

FIGURE 10: Subpicosecond time-resolved absorption spectra of the intact and reassembled chlorosomes (see the materials and methods for the experimental details). Stimulated emission from the Soret and the Q_y singlet states as well as transient absorption from the triplet (T_1) state is seen. The spectral changes can be explained in terms of singlet homofission followed by triplet−triplet annihilation (see the text for the detailed mechanisms).

(730 nm) than the Q_y emission (770 nm). (iii) After the vibrational relaxation from the former to the latter, only the stimulated emission from the relaxed Q_y state (770 nm) remains.

In a previous investigation (*21*), we examined the excited-state dynamics in the intact and variously modified chlorosomes from *Chl. tepidum* and identified the same sequence of excited-state reactions, i.e., the singlet−homofission reaction to generate the T_1 state followed by the triplet−triplet annihilation reaction to cause triplet-to-singlet transformation (see Scheme C in Figure 3 in ref *21*), i.e., exactly the same excited-state reactions mentioned above.

In the previous investigation, we excited the intact chlorosomes from *Chl. tepidum* at 397 nm with a photon density of 4×10^{14} photon·cm^{-2}·pulse^{-1}, whereas in the present investigation, we excited the intact and reassembled chlorosomes from *Chl. limicola* at 454 and 455 nm with a photon density of 2.6×10^{14} photon·cm^{-2}·pulse^{-1}. A clear difference is in the wavelength of excitation. As a result, in the present time-resolved spectra shown in Figure 10, the above pair of excited-state reactions is seen much more clearly than the previous time-resolved spectra (Figure 4 of ref *21*). In particular, the hot Q_y state to be generated immediately after the triplet−triplet annihilation is clearly seen at 736 nm, in the present investigation, most probably due to the excitation exactly on the Soret absorption peak (454−455 nm). It is well documented that the broad "Soret" absorption is actually an overlap of various electronic transitions (*36*).

Thus, the subpicosecond time-resolved spectra in the intact and reassembled chlorosomes are very similar to each other, indicating that the excited-state dynamics in the BChl *c* aggregates in those rod elements are basically the same, although the hot Q_y state absorption (the shoulder) is more clearly seen in the intact chlorosomes than the reassembled chlorosomes.

It is to be noted that the singlet−homofission and triplet−triplet annihilation reactions we identified in subpicosecond time-resolved absorption spectroscopy are relevant to the photoprotective function of the BChl *c* aggregates in the rod elements: It has been well documented that the aggregate structure of BChl *c* prevents the generation of singlet oxygen. More precisely, in the monomeric state, singlet oxygen can be efficiently generated sensitized by the triplet-state BChl *c*, while singlet oxygen can be efficiently quenched by the ground-state BChl *c* (*37*). The pair of results suggests that the energy of triplet BChl *c* is similar to that of singlet oxygen. However, it was found that the yield of singlet oxygen by the photoexcitation of dimeric BChl *c* is 6 times less than that by monomeric BChl *c*. Further, the sensitized generation of singlet oxygen was not observed at all in the oligomer-containing solution or in chlorosomes (*38*). Thus, the BChl *c* aggregates itself can be considered to be a photoprotective system against the singlet oxygen formation.

Similar observation has been reported in BChl *e* (*39*): In Ar-purged acetone (in the monomeric state), triplet BChl *e* has a lifetime of a few tens of microseconds. In air-saturated acetone, the quenching of BChl *e* by ground-state oxygen and the formation of singlet oxygen took place with a quantum yield of 0.65. The resultant singlet oxygen was susceptible to quenching by ground-state BChl *e*. However, no sensitized generation of singlet oxygen was observed at all in the aggregates.

The above experimental observation, i.e., no sensitized generation of singlet oxygen in aggregates and in chlorosomes containing BChl *c* or *e*, can be nicely explained in terms of our observation that such triplet−triplet annihilation reaction can take place within 10−20 ps as shown in Figure 10; then, there is no chance of the BChl-sensitized generation of singlet oxygen that is diffusion limited.

(i) The Rod Model or the Lamellar Model. The present characterization of "the reassembled chlorosomes" is based on the traditional picture of chlorosomes consisting of the rod elements (cylindrical aggregates) enveloped by a monolayer of MGDG. Here, we call this "the rod model". We used a set of experimental techniques, (a)−(h), for comparison of the intact and reassembled chlorosomes. No observations contradictory to the rod model were obtained. The electron micrographs (Figure 3) support the spheroidal structure of chlorosomes, and the zeta potential data support the idea that the rod elements were enveloped by the MGDG monolayer. The inset of the electron micrograph exhibits rod-like structures, a fact which is consistent to the electron

micrograph showing the rod elements coming out from a punctured chlorosome (*8*). More microscopically, the CD pattern of the Q_y absorption exhibiting the (−, +, −) signs can be explained by the cylindrical arrangement of transition dipoles, the direction of which are tilted with respect to the long axis.

In order to establish the rod model, however, more detailed morphological analysis of the rod elements by electron microscopy is absolutely necessary. It is also important how to build a model for the rod elements containing a large amount of water molecules and giving rise to the X-ray diffraction peak at 23.8 Å (Figure 9).

The lamellar model, on the other hand, is much less characterized. It is most important to show what are seen by electron micrograph are *not* the rod elements *but* the wavy lamellars. Here again, it is necessary to establish the assignment of the electron diffraction peak at ∼20 Å. It is important that the electron micrographs were taken for chlorosomes with vitreous ice. As we experienced in the present investigation, water molecules play an important role in keeping the intact structure of chlorosomes.

It is to be emphasized that the aggregate structure probed by ^{13}C NMR as well as by CD and stationary-state and subpicosecond time-resolved electronic absorption spectroscopies is rather in a short range (or too microscopic), when compared to the sizes of the rod elements and the entire chlorosome. In other words, such a short-range structure is applicable either to the rod model or to the lamellar model.

In summary, whether the rod model or the lamellar model is still an open question.

CONCLUSION

The following answers to the questions addressed in the introduction have been obtained on the basis of a set of experimental results.

Question 1: How can the morphology of the reassembled chlorosomes be characterized in comparison to the intact chlorosomes? (a) Densities determined by sucrose density gradient centrifugation: The intact chlorosomes showed densities in the range of 1.15−1.17 g·cm^{-3} (centered around 1.16 g·cm^{-3}), whereas the reassembled chlorosomes, a density of 1.15 g·cm^{-3}. The broad range of density seen in the intact chlorosomes was ascribed to the inhomogeneous isomeric and epimeric composition, reflecting the varying light intensity during the cell growth in a Rue bottle due to the self-shadowing effect. (b) Surface charges as determined by zeta-potential: The excellent agreement in the maxima of the zeta potential profiles between the intact and reassembled chlorosomes strongly suggested that the BChl *c* aggregates to form the rod elements were enveloped by the same MGDG lipid monolayer. (c) Structures observed by transmission electron microscopy: The shape of the intact chlorosomes was a round and smooth spheroid, whereas that of the reassembled chlorosomes was an elongated spheroid forming a spiral. The size of the reassembled chlorosomes (175 nm × 50 nm) was much larger than that of the intact chlorosomes (100 nm × 40 nm). (d) Size distributions determined by dynamic light scattering: The diameter at the maximum population, calculated by assuming a spherical structure, was ∼80 nm in the intact chlorosomes, while it was ∼190 nm in the reassembled chlorosomes.

Question 2: How can the BChl *c* aggregates forming the rod elements be characterized in comparison to those in the intact chlorosomes? Can any conclusion be drawn concerning the monomer-based or dimer-based stacking by the use of the set of data obtained? (e) ^{13}C magnetic dipole interactions probed by solid-state NMR spectroscopy: Most of the correlation peaks from the intact and reassembled chlorosomes (both 100% ^{13}C-BChl *c*) were similar to each other, suggesting that the stackings of the macrocycles were basically the same. Importantly, large splittings of the C5 signals in the 2d DARR spectra clearly showed that BChl *c* aggregates in the rod elements, in the intact and reassembled chlorosomes, consisted of the piggy-back dimers. (f) Interactions among the Q_y transition dipoles probed by electronic absorption and CD spectroscopies: The overall electronic absorption and CD spectral patterns were very similar to each other in the intact and reassembled chlorosomes, indicating that the pigment assemblies were basically the same. (g) Regular atomic arrangements probed by low-angle X-ray diffraction: The diffraction patterns of the intact and reassembled chlorosomes were indistinguishable, which indicated that the *regular* atomic arrangements were identical. This technique revealed that the water content was the key to reproduce the particular diffraction pattern and, as a result, the chlorosome structure.

Question 3: How can the excited-state dynamics be characterized? Can any relevance be found concerning the light-harvesting or photoprotective function of chlorosomes? (h) Excited-state dynamics probed by time-resolved absorption spectroscopy: The subpicosecond time-resolved absorption spectra of the intact and reassembled chlorosomes were very similar to each other, indicating that the excited-state dynamics in the BChl *c* aggregates in the rod elements were basically the same. The time-resolved spectra exhibited the excited-state dynamics including singlet homofission followed by triplet−triplet annihilation, which turned out to be relevant to the photoprotective function. Previous experimental observations, i.e., no sensitized generation of singlet oxygen in BChl *c* and *e* aggregates and in chlorosomes, could be nicely explained in terms of our finding in the present investigation, i.e., the extremely efficient triplet−triplet annihilation reaction taking place within 10−20 ps; in this time range, there is no chance of sensitized generation of singlet oxygen that is diffusion limited.

Most importantly, we have succeeded in the preparation of the reassembled chlorosomes containing ^{13}C-BChl *c* and ^{12}C-BChl *c* in a 1:1 ratio in the lipid envelope and the extraction of the intermolecular $^{13}C\cdots{}^{13}C$ magnetic dipole correlation peaks as shown in Figure 5 (lower panels). We have already started the analysis of PDSD and DARR spectra of the reassembled chlorosomes containing 100% and 50% ^{13}C-BChl *c*. Hopefully, we will be able to determine the assembly of BChl *c* in the aggregates forming the rod elements in the reassembled chlorosomes in the near future.

ACKNOWLEDGMENT

We thank Mr. Yoshio Kawakami and Mr. Shoichi Nakamura (Otsuka Electronics Co. Ltd., Japan) for measuring the zeta potential and size distribution, Dr. Eiko Nakazawa (Hitachi High-Technologies Corp., Japan) for taking electron micrographs, Mr. Hiroaki Utsumi and Mr. Yuichi Shi-

moikeda (JEOL Ltd., Japan) for measuring the DARR spectra, and Mr. Hiroshi Yoshioka (Kwansei Gakuin University, Japan) for experimental support, specially making a housing in X-ray diffraction measurements keeping the hygroscopic condition.

REFERENCES

1. Blankenship, R. E., and Matsuura, K. (2003) Antenna Complexes from Green Photosynthetic Bacteria, in *Light-Harvesting Antennas in Photosynthesis* (Green, B. R., and Parson, W. W., Eds.) pp 195−217, Kluwer Academic Publishers, Dordrecht, The Netherlands.
2. Olson, J. M. (1998) Chlorophyll organization and function in green photosynthetic bacteria, *Photochem. Photobiol. 67*, 61−75.
3. Blankenship, R. E., Olson, J. M., and Miller, M. (1995) Antenna Complexes from Green Photosynthetic Bacteria, in *Anoxygenic Photosynthetic Bacteria* (Blankenship, R. E., Madigan, M. T., and Bauer, C. E., Eds.) pp 399−435, Kluwer Academic Publishers, Dordrecht, The Netherlands.
4. Oelze, J., and Golecki, J. R. (1995) Membranes and Chlorosomes of Green Bacteria: Structure, Composition and Development, in *Anoxygenic Photosynthetic Bacteria* (Blankenship, R. E., Madigan, M. T., and Bauer, C. E., Eds.) pp 259−278, Kluwer Academic Publishers, Dordrecht, The Netherlands.
5. Cohen-Bazire, G., Pfennig, N., and Kunisawa, R. (1964) The fine structure of green bacteria, *J. Cell Biol. 22*, 207−225.
6. Staehelin, L. A., Golecki, J. R., Fuller, R. C., and Drews, G. (1978) Visualization of the supramolecular architecture of chlorosomes (*Chlorobium* type vesicles) in freeze-fractured cells of *Chloroflexus aurantiacus*, *Arch. Microbiol. 119*, 269−277.
7. Staehelin, L. A., Golecki, J. R., and Drews, G. (1980) Supramolecular organization of chlorosomes (*Chlorobium* vesicles) and of their membrane attachment sites in *Chlorobium limicola*, *Biochim. Biophys. Acta 589*, 30−45.
8. Wullink, W., and van Bruggen, E. F. J. (1988) Structural Studies on Chlorosomes from *Prosthecochloris aestuarii*, in *Green Photosynthetic Bacteria* (Olson, J. M., Ormerod, J. G., Amesz, J., Stackebrandt, E., and Trüper, H. G., Eds.) pp 3−14, Plenum Press, New York.
9. Martinez-Planells, A., Arellano, J. B., Borrego, C. M., López-Iglesias, C., Gich, F., and Garcia-Gil, J. (2002) Determination of the topography and biometry of chlorosomes by atomic force microscopy, *Photosynth. Res. 71*, 83−90.
10. Montaño, G. A., Bowen, B. P., LaBelle, J. T., Woodbury, N. W., Pizziconi, V. B., and Blankenship, R. E. (2003) Characterization of *Chlorobium tepidum* chlorosomes: A calculation of bacteriochlorophyll *c* per chlorosome and oligomer modeling, *Biophys. J. 85*, 2560−2565.
11. Pšenčík, J., Ikonen, T. P., Laurinmäki, P., Merckel, M. C., Butcher, S. J., Serimaa, R. E., and Tuma, R. (2004) Lamellar organization of pigments in chlorosomes, the light harvesting complexes of green photosynthetic bacteria, *Biophys. J. 87*, 1165−1172.
12. Balaban, T. S., Linke-Schaetzel, M., Bhise, A. D., Vanthuyne, N., Roussel, C., Anson, C. E., Buth, G., Eichhöfer, A., Foster, K., Garab, G, Gliemann, H., Goddard, R., Javorfi, T., Powell, A. K., Rösner, H., and Schimmel, T. (2005) Structural characterization of artificial self-assembling porphyrins that mimic the natural chlorosomal bacteriochlorophylls *c*, *d*, and *e*, *Chem. Eur. J. 11*, 2267−2275.
13. Holzwarth, A. R., and Schaffner, K. (1994) On the structure of bacteriochlorophyll molecular aggregates in the chlorosomes of green bacteria. A molecular modelling study, *Photosynth. Res. 41*, 225−233.
14. van Rossum, B.-J., Steensgaard, D. B., Mulder, F. M., Boender, G. J., Schaffner, K., Holzwarth, A. R., and de Groot, H. J. M. (2001) A refined model of the chlorosomal antennae of the green bacterium *Chlorobium tepidum* from proton chemical shift constraints obtained with high-field 2-D and 3-D MAS NMR dipolar correlation spectroscopy, *Biochemistry 40*, 1587−1595.
15. Nozawa, T., Ohtomo, K., Suzuki, M., Morishita, Y., and Madigan, M. T. (1993) Structures and organization of bacteriochlorophyll *c*'s in chlorosomes from a new thermophilic bacterium *Chlorobium tepidum*, *Bull. Chem. Soc. Jpn. 66*, 231−237.
16. Nozawa, T., Ohtomo, K., Suzuki, M., Nakagawa, H., Shikama, Y., Konami, H., and Wang, Z.-Y. (1994) Structures of chlorosomes and aggregated BChl *c* in *Chlorobium tepidum* from solid state high resolution CP/MAS ^{13}C NMR, *Photosynth. Res. 41*, 211−223.
17. Kakitani, Y., Nagae, H., Mizoguchi, T., Egawa, A., Akiba, K., Fujiwara, T., Akutsu, H., and Koyama, Y. (2006) Assembly of a mixture of isomeric BChl *c* from *Chlorobium limicola* as determined by intermolecular ^{13}C−^{13}C dipolar correlations: Coexistence of dimer-based and pseudo-monomer-based stackings, *Biochemistry 45*, 7574−7585.
18. Hirota, M., Moriyama, T., Shimada, K., Miller, M., Olson, J. M., and Matsuura, K. (1992) High degree of organization of bacteriochlorophyll *c* in chlorosome-like aggregates spontaneously assembled in aqueous solution, *Biochim. Biophys. Acta 1099*, 271−274.
19. Wahlund, T. M., Woese, C. R., Castenholz, R. W., and Madigan, M. T. (1991) A thermophilic green sulfur bacterium from New Zealand hot springs, *Chlorobium tepidum* sp. nov., *Arch. Microbiol. 156*, 81−90.
20. Gerola, P. D., and Olson, J. M. (1986) A new bacteriochlorophyll *a*-protein complex associated with chlorosomes of green sulfur bacteria, *Biochim. Biophys. Acta 848*, 69−76.
21. Kakitani, Y., Rondonuwu, F. S., Mizoguchi, T., Watanabe, Y., and Koyama, Y. (2003) Energy dissipations in chlorosomes: Emission from the Q_y state following singlet−singlet and triplet-triplet annihilation reactions in the cylindrical aggregate and its reversible dissociation into the piggy-back dimers, *J. Phys. Chem. B 107*, 14545−14555.
22. Takegoshi, K., Nakamura, S., and Terao, T. (2003) ^{13}C−^{1}H dipolar-driven ^{13}C−^{13}C recoupling without ^{13}C rf irradiation in nuclear magnetic resonance of rotating solids, *J. Chem. Phys. 118*, 2325−2341.
23. Borrego, C. M., Gerola, P. D., Miller, M., and Cox, R. P. (1999) Light intensity effects on pigment composition and organisation in the green sulfur bacterium *Chlorobium tepidum*, *Photosynth. Res. 59*, 159−166.
24. Senge, M. O., and Smith, K. M. (1995) Biosynthesis and Structures of the Bacteriochlorophylls, in *Anoxygenic Photosynthetic Bacteria* (Blankenship, R. E., Madigan, M. T., and Bauer, C. E., Eds.) pp 137−151, Kluwer Academic Publishers, Dordrecht, The Netherlands.
25. Frigaard, N.-U., Chew, A. G. M., Li, H., Maresca, J. A., and Bryant, D. A. (2003) *Chlorobium tepidum*: Insights into the structure, physiology, and metabolism of a green sulfur bacterium derived from the complete genome sequence, *Photosynth. Res. 78*, 93−117.
26. Mizoguchi, T., Ogura, K., Inagaki, F., and Koyama, Y. (1999) The structure of an aggregate form of bacteriochlorophyll *c* showing the Q_y absorption at 705 nm as determined by the ring-current effects on ^{1}H and ^{13}C nuclei and by ^{1}H−^{1}H intermolecular NOE correlations, *Biospectroscopy 5*, 63−77.
27. Mizoguchi, T., Hara, K., Nagae, H., and Koyama, Y. (2000) Structural transformation among the aggregate forms of bacteriochlorophyll *c* as determined by electronic-absorption and NMR spectroscopies: Dependence on the stereoisomeric configuration and on the bulkiness of the 8-C side chain, *Photochem. Photobiol. 71*, 596−609.
28. Mizoguchi, T., Matsuura, K., Shimada, K., and Koyama, Y. (1996) The structure of the aggregate form of bacteriochlorophyll *c* showing the Q_y absorption above 740 nm: A ^{1}H-NMR study, *Chem. Phys. Lett. 260*, 153−158.
29. Mizoguchi, T., Sakamoto, S., Koyama, Y., Ogura, K., and Inagaki, F. (1998) The structure of the aggregate form of bacteriochlorophyll *c* showing the Q_y absorption above 740 nm as determined by the ring-current effects on ^{1}H and ^{13}C nuclei and by the ^{1}H−^{1}H intermolecular NOE correlations, *Photochem. Photobiol. 67*, 239−248.
30. Steensgaard, D. B., Wackerbarth, H., Hildebrandt, P., and Holzwarth, A. R. (2000) Diastereoselective control of bacteriochlorophyll *e* aggregation. 3^{1}-*S*-BChl *e* is essential for the formation of chlorosome-like aggregates, *J. Phys. Chem. B 104*, 10379−10386.
31. Pšenčík, J., Arellano, J. B., Ikonen, T. P., Borrego, C. M., Laurinmäki, P. A., Butcher, S. J., Serimaa, R. E., and Tuma, R. (2006) Internal structure of chlorosomes from brown-colored *Chlorobium* species and the role of carotenoids in their assembly, *Biophys. J. 91*, 1433−1440.
32. Griebenow, K., Holzwarth, A. R., van Mourik, F., and van Grondelle, R. (1991) Pigment organization and energy transfer in green bacteria. 2. Circular and linear dichroism spectra of protein-containing and protein-free chlorosomes isolated from

Chloroflexus aurantiacus strain Ok-70-fl, *Biochim. Biophys. Acta 1058*, 194−202.

33. Wang, Z.-Y., Marx, G., Umetsu, M., Kobayashi, M., Mimuro, M., and Nozawa, T. (1995) Morphology and spectroscopy of chlorosomes from *Chlorobium tepidum* by alcohol treatments, *Biochim. Biophys. Acta 1232*, 187−196.
34. Prokhorenko, V. I., Steensgaard, D. B., and Holzwarth, A. R. (2003) Exciton theory for supramolecular chlorosomal aggregates: 1. Aggregate size dependence of the linear spectra, *Biophys. J. 85*, 3173−3186.
35. Didraga, C., and Knoester, J. (2004) Optical spectra and localization of excitons in inhomogeneous helical cylindrical aggregates, *J. Chem. Phys. 121*, 10687−10698.
36. Petke, J. D., Maggiora, G. M., Shipman, L., and Christoffersen, R. E. (1979) Stereoelectronic properties of photosynthetic and related systems−V. *ab initio* Configutation interaction calculations on the ground and lower excited singlet and triplet states of ethyl chlorophyllide *a* and ethyl pheophorbide *a*, *Photochem. Photobiol. 30*, 203−223.
37. Krasnovsky, A. A., Jr., Cheng, P., Blankenship, R. E., Moore, T. A., and Gust, D. (1993) The photophysics of monomeric bacteriochlorophylls *c* and *d* and their derivatives: Properties of the triplet state and singlet oxygen photogeneration and quenching, *Photochem. Photobiol. 57*, 324−330.
38. Krasnovsky, A. A., Jr., Lopez, J., Cheng, P., Liddell, P. A., Blankenship, R. E., Moore, T. A., and Gust, D. (1994) Generation and quenching of singlet molecular oxygen by aggregated bacteriochlorophyll *d* in model systems and chlorosomes, *Photosynth. Res. 40*, 191−198.
39. Arellano, J. B., Melø, T. B., Borrego, C. M., and Naqvi, K. R. (2002) Bacteriochlorophyll *e* monomers, but not aggregates, sensitize singlet oxygen: Implications for a self-photoprotection mechanism in chlorosomes, *Photochem. Photobiol. 76*, 373−380.

BI602586G